Nature of Perpendicular-to-Parallel Spin Reorientation in a Mn-doped GaAs Quantum Well: Canting or Phase Separation?

Randy S. Fishman,[1] Fernando A. Reboredo,[1] Alex Brandt,[1,2] and Juana Moreno[3]

[1]*Materials Science and Technology Division, Oak Ridge National Laboratory, Oak Ridge, Tennessee 37831-6065, USA*
[2]*Department of Physics and Astronomy, Minnesota State University Moorhead, Moorhead, Minnesota 56563, USA*
[3]*Physics Department, University of North Dakota, Grand Forks, North Dakota 58202-7129, USA*

(Received 8 January 2007; published 27 June 2007)

It is well known that the magnetic anisotropy in a compressively strained Mn-doped GaAs film changes from perpendicular to parallel with increasing hole concentration p. We study this reorientation transition at $T = 0$ in a quantum well with delta-doped Mn impurities. With increasing p, the angle θ that minimizes the energy E increases continuously from 0 (perpendicular anisotropy) to $\pi/2$ (parallel anisotropy) within some range of p. The shape of $E^{\min}(p)$ suggests that the quantum well becomes phase separated with regions containing low hole concentrations and perpendicular moments interspersed with other regions containing high hole concentrations and parallel moments. However, because of the Coulomb energy cost associated with phase separation, the true magnetic state in the transition region is canted with $0 < \theta < \pi/2$.

DOI: 10.1103/PhysRevLett.98.267203 PACS numbers: 75.50.Pp, 73.61.Ey, 75.30.Gw

During the past decade, the ferromagnetic transition temperature of Mn-doped GaAs films has been quickly approaching room temperature [1]. Theoretical studies of Mn-doped GaAs [2] based on the Kohn-Luttinger (KL) model have been quite successful at modeling and predicting much of the behavior found experimentally. In agreement with theory [3,4], experiments show that at low temperatures, the magnetic anisotropy of films under compressive strain is perpendicular or out of the plane when the hole concentration p is small, transforming to parallel or in the plane as p increases [5]. Although GaAs quantum wells with delta-doped Mn impurities have also been studied theoretically for several years [6,7], little is known about the nature of the spin reorientation in those systems. We show that the spin reorientation in a delta-doped quantum well happens in three stages: for small hole concentrations, the angle θ of the magnetization with respect to the film normal is 0 so that the magnetization lies perpendicular to the plane; for high hole concentrations, $\theta = \pi/2$ so that the magnetization lies in the plane of the quantum well. In between, the moments are either canted with $0 < \theta < \pi/2$ or phase-separated with regions containing low hole concentrations and perpendicular moments interspersed with regions containing high hole concentrations and parallel moments.

The magnetic anisotropy of a quantum well sensitively depends on the spin-orbit coupling. In pure GaAs, the spin-orbit coupling plays two roles. First, it lowers the energy of the $j = 1/2$ band compared to the $j = 3/2$ band at the Γ point by about 320 meV. Since the lower $j = 1/2$ band is rarely occupied by any holes, it is commonly ignored. Second, spin-orbit coupling changes the energies of the $j = 3/2$ holes so that heavy ($m_h = 0.5m$) and light ($m_l = 0.07m$) holes carry angular momentum $\mathbf{j} \cdot \hat{\mathbf{k}} = \pm 3/2$ and $\pm 1/2$, respectively, along their momentum direction $\hat{\mathbf{k}}$. In the absence of elastic strain, the energies of the light and heavy hole bands in bulk GaAs are degenerate at the Γ point.

In a quantum well bounded by $z = \pm L/2$, the square of the z component of the momentum is quantized. For the two lowest wave functions $\psi_1(z) = \sqrt{2/L}\cos(\pi z/L)$ and $\psi_2(z) = \sqrt{2/L}\sin(2\pi z/L)$ of the quantum well, $\langle n|k_z^2|m\rangle = (n\pi/L)^2\delta_{nm}$. Because of the difference between the light and heavy hole masses, the confinement of the holes in a quantum well breaks the degeneracy of the $j = 3/2$ bands at the Γ point with $\mathbf{k}_\perp = 0$. To simplify the following discussion, we shall discuss hole rather than electron bands so that hole energies increase quadratically like $k_\perp^2$ for small $k_\perp$. Including the effects of lattice strain, the energy gap between the $j_z = \pm 3/2$ and $\pm 1/2$ subbands of $\psi_n(z)$ at the Γ point is

$$\Delta_n = \frac{\langle n|k_z^2|n\rangle}{2}\left\{\frac{1}{m_l} - \frac{1}{m_h}\right\} - 2b_d Q_\epsilon, \tag{1}$$

where $Q_\epsilon = \epsilon_{zz} - (\epsilon_{xx} + \epsilon_{yy})/2$ and $b_d \approx -1.6$ eV is the deformation potential [4]. Hence, compressive strain ($Q_\epsilon > 0$) plays qualitatively the same role as carrier confinement within the quantum well.

For a quantum well with 20 or fewer layers, the contribution of strain (typically less than 0.5% [8]) to the band splittings Δ_n can be safely neglected compared to that of carrier confinement. On the other hand, the main contribution to the band splitting in homogeneously-doped GaAs films comes from strain [3,8] rather than the confinement of the holes. For delta-doped GaAs quantum wells with more than 20 layers, the Coulomb potential exerted on the holes [9] by the single layer of Mn impurities will lower the effective width of the quantum well so that confinement again provides the dominant contribution to Δ_n. Hence, our model should apply to most quantum-well structures with a

narrow layer of Mn impurities. As shown recently [10], the energy splittings Δ_n produce a gap in the spin-wave spectrum that allows a two-dimensional layer of Mn spins to order ferromagnetically.

The carriers in the lower, $j_z = \pm 3/2$, and upper, $j_z = \pm 1/2$, subbands have bandmasses $m_a = 0.089m$ and $m_b = 0.197m$, respectively, where $4/m_a = 3/m_l + 1/m_h$ and $4/m_b = 1/m_l + 3/m_h$ [4,10]. The coupling of the $j = 3/2$ holes with the Mn spins is included by treating the $S = 5/2$ Mn spins classically and by assuming that Mn impurities with concentration c are restricted to the $z = 0$ plane. We shall denote p as the number of holes for each of the N cations in the central plane. For small p, the holes occupy a small portion of the $\mathbf{k}_\perp$ Brillouin zone centered around $\mathbf{k}_\perp = 0$. Since the holes then interact with many different Mn moments, the precise locations and structure of the Mn impurities are not important, and their interactions with the holes may be treated within a mean-field approximation. The exchange coupling of the Mn spins $\mathbf{S}_i = S\mathbf{m}_i$ with the holes is then given by $V = -2J_c \sum_i \mathbf{m}_i \cdot \mathbf{j}_i$, where $\mathbf{j}_i$ are the hole spins and the sum is over all Mn sites. Comparing V with the potential used in Refs. [3,4], we obtain the exchange coupling $J_c = (S/4j)\beta N_0 2c/\Lambda$, where $\beta N_0 \approx 1.2$ eV is estimated from photoemission measurements [11] and $\Lambda = L/b$ is the number of layers in the quantum well. Here, $b \approx 4$Å is the Ga lattice constant in the $z = 0$ plane. It follows that $J_c \approx 1c/\Lambda$ eV.

While our results are supported by numerical calculations that include both wave functions $\psi_1(z)$ and $\psi_2(z)$, a qualitative understanding of the magnetic anisoptropy can be obtained from a simplified model that considers only $\psi_1(z)$. Because of the typically small Mn concentrations, the demagnetization fields can be neglected compared to the anisotropy introduced by the electronic band structure. If the Mn moments are tilted an angle θ away from the z axis, then to linear order in J_c, the two lower subbands are split by $\pm 3J_c$ ($\theta = 0$) or 0 ($\theta = \pi/2$), as shown in Fig. 1 for $\Lambda = 10$. By contrast, the two upper bands are split by $\pm J_c$ ($\theta = 0$) or $\pm 2J_c$ ($\theta = \pi/2$). When only the lowest subband is populated by holes, the energy difference $[E(\theta = 0) - E(\theta = \pi/2)]/N$ is of order $-J_c$ so that the anisotropy is perpendicular. When the two lower subbands

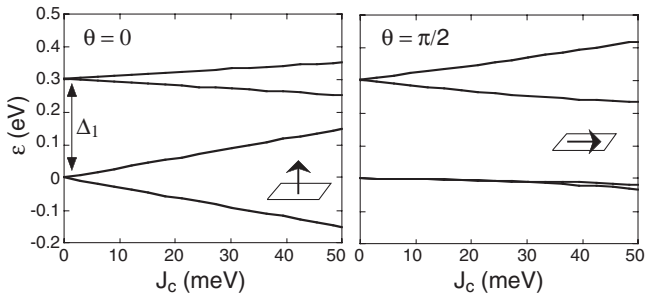

FIG. 1. The energies of the bottom of the carrier bands with $\mathbf{k}_\perp = 0$ versus J_c when only $\psi_1(z)$ is considered. The chemical potential increases with the hole filling.

are both occupied by holes, the energy difference is of order $-J_c^2 mb^2/c$ because more holes occupy the lowest subband and perpendicular anisotropy still dominates. But when holes begin to occupy the lower of the two upper subbands, the energy difference becomes positive and of order J_c due to the larger splitting of the upper subbands when $\theta = \pi/2$. Assuming that $J_c \ll \Delta_1$, the reorientation transition occurs close to the filling where the chemical potential $\mu \sim p/(b^2 m)$ crosses $\Delta_1 \sim 1/(b^2 \Lambda^2 m)$. Very roughly, this implies that the transition from perpendicular to parallel anisotropy occurs when $p \sim 1/\Lambda^2$, independent of the Mn concentration.

The scenario of magnetic reorientation would be reversed when tensile strain overcomes the effects of carrier confinement so that $\Delta_1 < 0$. Because perpendicular or parallel anisotropy dominates for compressive or tensile strain only at very low hole concentrations, the behavior of the anisotropy at higher hole concentrations has led to the often-repeated statement [12] that compressive or tensile strain is associated with parallel or perpendicular anisotropy.

We now examine more closely the details of the spin reorientation. With both wave functions $\psi_1(z)$ and $\psi_2(z)$ included, there are 8 hole bands rather than 4 for every $\mathbf{k}_\perp$ point. Since $\psi_2(0) = 0$, the Mn spins only couple to the holes in $\psi_1(z)$, with projection $|\psi_1(0)|^2 = 2/L$. The wave functions $\psi_1(z)$ and $\psi_2(z)$ are coupled by the off-diagonal terms in the KL Hamiltonian with matrix elements proportional to $\langle n|(k_x \pm ik_y)k_z|m\rangle$, which vanishes for $n = m$ but is given by $-(8i/3L)(k_x \pm ik_y)$ for $n = 1$ and $m = 2$. The energy $E(J_c, \theta)$ of the KL plus exchange (KLE) model is obtained by first diagonalizing the Hamiltonian written as an 8 by 8 matrix in $j = 3/2$ and $n, m = 1, 2$ space. The resulting eigenvalues are integrated over $\mathbf{k}_\perp$ up to the Fermi level [10].

Fixing c and p, the energy E is then minimized with respect to θ. For $c = 0.4$, $E^{\min}/N$ is plotted versus p in Fig. 2. As shown, the angle θ corresponding to the minimum energy smoothly increases from 0 at $p_1 = 0.0128$ to $\pi/2$ at $p_2 = 0.019$. We have plotted p versus chemical potential $\mu = (1/N)dE^{\min}/dp$ in the inset to Fig. 2. This "S" shaped curve is typical of phase separation, where regions of different $\{\theta, p\}$ coexist. The phase with high or low hole density is metastable so long as $d^2E^{\min}/dp^2 > 0$ or $dp/d\mu > 0$, while the phase is unstable when $dp/d\mu < 0$. Performing a Maxwell construction for the data in Fig. 2, we find that phase separation occurs between regions with hole concentration $p_l = 0.0113 < p_1$ and $\theta = 0$ and regions with $p_u = 0.02 > p_2$ and $\theta = \pi/2$. The phase-separated region is bracketed by the solid circles in Fig. 2. As the hole concentration increases from p_l to p_u, the total area of the regions with parallel or perpendicular anisotropy increases or decreases, respectively. A phase-separated phase is stable only if the KLE Hamiltonian is expanded in more than one $\psi_n(z)$.

However, phase separation of the quantum well into regions with low and high hole concentrations costs

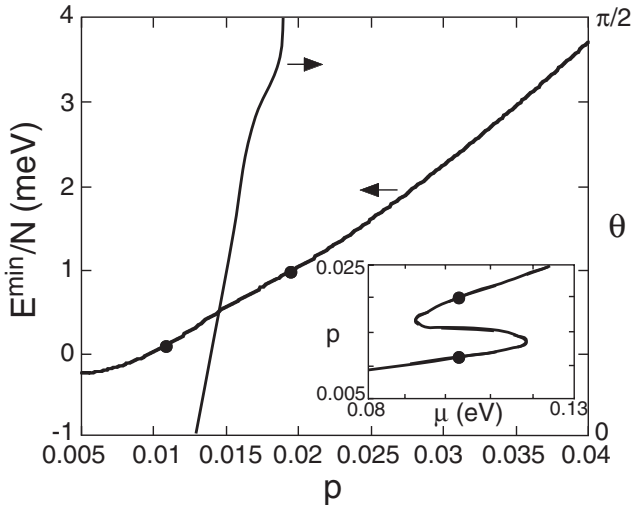

FIG. 2. The minimum energy $E^{\min}/N$ and the angle θ versus p for $c = 0.4$ and $\Lambda = 10$. Inset is a plot of p versus μ, revealing an "S" shaped curve. A Maxwell construction yields phase separation between the two solid circles.

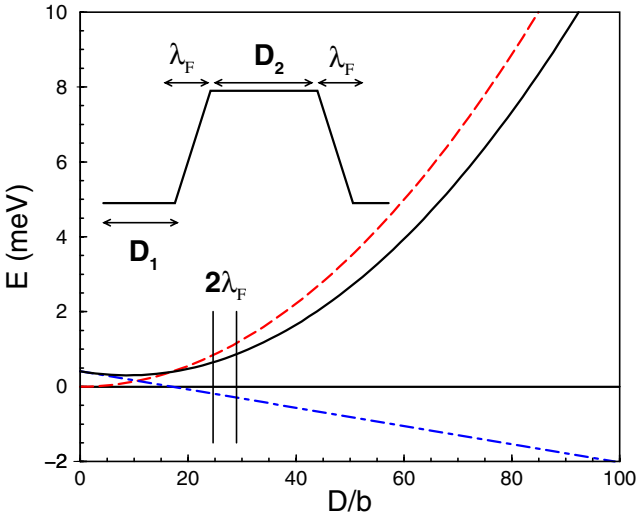

FIG. 3 (color online). The total energy gain of a phase-separated mixture (dot-dashed curve), the Coulomb cost associated with the domain wall (dashed curve), and the total energy when both contributions are added (solid curve) versus the size of the region for $c = 0.5$ and $\Lambda = 10$. The higher and lower values of $2\lambda_F$ are associated with perpendicular and parallel Mn moments, respectively. The results below $2\lambda_F$ have no physical meaning since D_1 and D_2 would have to be negative.

Coulomb energy, which was not taken into account by the KLE model. The size of the phase-separated regions will be determined by a balance between the cost in Coulomb energy and the energy gained by phase separation. The Coulomb and phase-separation energies are estimated by supposing that a charge-density wave in the Mn plane oscillates between fillings p_l and p_u within a rectangular region in the $z = 0$ plane of length D and width b. As described in the inset to Fig. 3, a region of length D_1 and filling p_l and a region of length D_2 and filling p_u are separated by an interface of length λ_F. The total length of the rectangular region is $D = D_1 + D_2 + 2\lambda_F$, which is measured in units of the in-plane lattice constant b. For overall filling p, charge conservation requires that $pD = p_l D_1 + p_u D_2 + \lambda_F(p_l + p_u)$.

To calculate the energy gained by creating a phase-separated mixture, we subtract the energy of a uniform phase with $p = (p_l + p_u)/2$, yielding the dot-dashed curve in Fig. 3 [13]. The dielectric constant for GaAs is used to evaluate the Coulomb energy cost, given by the dashed curve in Fig. 3. The Fermi wavelength $\lambda_F = 2\pi/k_F$ is evaluated for this uniform filling p with both Mn orientations. While the perpendicular k_F is a bit smaller than the parallel k_F, the calculated total energies are both positive. We conclude that phase separation is prevented by the cost in Coulomb energy for $c = 0.5$ and that the Mn moments will be canted for fillings between p_1 and p_2. This is also the case for smaller Mn dopings which are slightly more unfavorable to phase separation. In the homogeneous phase with filling p, the canting angle θ is not affected by the Coulomb energy and $\theta(p)$ can be taken directly from our results.

Since the long-range electric field contribution to the Coulomb energy may be suppressed in a double quantum well, where the excess electronic charge on one quantum well is offset by the deficit on the other, a double quantum well may exhibit phase separation rather than canting. By tuning the distance between the individual quantum wells, it may be possible to control the transformation from canting to phase separation. The dependence of the hole density on the magnetization angle will induce a coupling between spin- and charge-density excitations analogous to the ones observed in electronic systems [14]. The emergence of phase separation will soften the transverse charge-density mode in a double quantum well.

In Fig. 4, we plot the phase diagram of the magnetic orientation in the quantum well, leaving open the possibility of phase separation. The canted region is just a bit narrower than the phase-separated region shown in the figure. The lower bound to the canted region is given fairly accurately by $p_1 \approx 0.012$ for all c. By contrast, the upper bound p_2 increases from 0.0135 at $c = 0.15$ to 0.018 at $c = 0.5$. Hence, both the phase-separated and canted regions grow as the Mn concentration increases.

Because of the large size of the gap energy Δ_1, we do not expect our results to change very much with increasing temperature so long as $T \ll \Delta_1 \approx 29/\Lambda^2$ eV. Bear in mind that the width of the effective quantum well cannot exceed the confining Coulomb potential exerted by the plane of Mn impurities [9]. When the Mn concentration $c(z)$ is distributed along the width of the quantum well, our results with effective Mn concentration $c_{\text{eff}} = (L/2) \times \int_{-L/2}^{L/2} dz |\psi_1(z)|^2 c(z)$ will be unchanged provided that $(L/2) \int_{-L/2}^{L/2} dz |\psi_2(z)|^2 c(z) \ll c_{\text{eff}}$. The relevant ingredients of the spin-reorientation transition are the single-

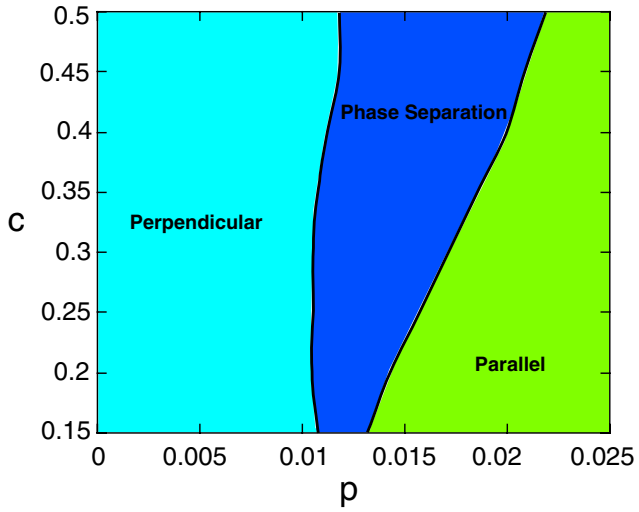

FIG. 4 (color online). The phase diagram of the magnetic orientation in a quantum well with $\Lambda = 10$, for Mn concentration c versus holes per cation p, showing regions of perpendicular and parallel anisotropy, as well as a possible phase-separated region.

particle gap Δ_1, the spin-orbit coupling in the valence band, and the magnetic coupling of the Mn ions with holes. These elements and not the confining potential control our results, which should apply to a wide range of realistic quantum wells.

Moving the Mn plane away from the center of the quantum well has interesting consequences. If the Mn plane is shifted to to $z' = \pm L/6$, then $|\psi_1(z')|^2 = |\psi_2(z')|^2$ so the Mn moments couple equally to the holes of both wave functions. For $c = 0.4$, the canted region between $p_1 = 0.048$ and $p_2 = 0.064$ is shifted substantially upwards by displacing the Mn plane.

Although the spin-reorientation transition has not been studied in a quantum well, several experiments have been performed on thin films. By measuring the remanent magnetization along different field directions, Sawicki *et al.* [5] estimated that the change from perpendicular to parallel magnetic anisotropy in 400 nm films with $c = 0.03$ or 0.05 occurs when $p \approx 10^{20}$ cm^{-3} or 0.0045 holes per cation. Using angle-dependent x-ray magnetic circular dichroism to study 50 nm films with $c = 0.02$ or 0.08, Edmonds *et al.* [15] observed this reorientation transition at a hole concentration of about 5 times higher or 0.0225 holes per cation.

The hole concentration in a quantum well may be controlled using a field-effect transistor, such as the one built by Ohno *et al.* [16]. Of course, the canting or phase separation of the Mn moments would be easier to observe if the spin-reorientation transition happened at higher values of p. As discussed above, the easiest way to enhance the hole filling of the spin reorientation in a narrow quantum well is to displace the Mn plane by 1/6 of the quantum-well width. We hope that this as well as our other predictions will encourage future measurements of the spin reorientation in quantum wells of delta-doped Mn.

This research was sponsored by the U.S. Department of Energy Division of Materials Science and Engineering under Contract No. DE-AC05-00OR22725 with Oak Ridge National Laboratory, managed by UT-Battelle, LLC. This research was also supported by NSF Grant Nos. DMR-0453518, DMR-0548011, EPS-0132289, and EPS-0447679. Research carried out in part at the University of North Dakota Computational Research Center, supported by NSF Nos. EPS-0132289 and EPS-0447679.

[1] T. Jungwirth *et al.*, Phys. Rev. B **72**, 165204 (2005).
[2] For a review of the theory of Mn-doped GaAs, see T. Jungwirth, J. Sinova, J. Mašek, J. Kučera, and A. H. MacDonald, Rev. Mod. Phys. **78**, 809 (2006).
[3] M. Abolfath, T. Jungwirth, J. Brum, and A. H. MacDonald, Phys. Rev. B **63**, 054418 (2001).
[4] T. Dietl, H. Ohno, and F. Matsukura, Phys. Rev. B **63**, 195205 (2001).
[5] M. Sawicki *et al.*, Phys. Rev. B **70**, 245325 (2004).
[6] L. Brey and F. Guinea, Phys. Rev. Lett. **85**, 2384 (2000).
[7] B. Lee, T. Jungwirth, and A. H. MacDonald, Phys. Rev. B **61**, 15606 (2000); J. König and A. H. MacDonald, Phys. Rev. Lett. **91**, 077202 (2003); D. Frustaglia, J. König, and A. H. MacDonald, Phys. Rev. B **70**, 045205 (2004).
[8] T. Dietl, J. König, and A. H. MacDonald, Phys. Rev. B **64**, 241201(R) (2001).
[9] F. A. Reboredo and C. R. Proetto, Phys. Rev. B **47**, 4655 (1993).
[10] R. G. Melko, R. S. Fishman, and F. A. Reboredo, Phys. Rev. B **75**, 115316 (2007).
[11] J. Okabayashi *et al.*, Phys. Rev. B **58**, R4211 (1998).
[12] A. Shen *et al.*, J. Cryst. Growth **175/176**, 1069 (1997); X. Liu, Y. Sasaki, and J. K. Furdyna, Phys. Rev. B **67**, 205204 (2003); L. Thevenard *et al.*, Phys. Rev. B **73**, 195331 (2006).
[13] The energy gained due to phase separation is

$$\Delta E_{\mathrm{PS}}(D) = \frac{2\lambda_F}{p_u - p_l}\int_{p_l}^{p_u} dp' E(p') + E(p_l)D_1 + E(p_u)D_2 - E(p)D.$$

In the unphysical limit $D \to 0$, D_1 and $D_2 \to -\lambda_F$ and $\Delta E_{\mathrm{PS}}(0) > 0$. Although the intercept $\Delta E_{\mathrm{PS}}(0)$ is proportional to λ_F, it hardly differs for the two possible values of λ_F for parallel or perpendicular moments, so their average is used to plot the dot-dashed curve in Fig. 3.
[14] P. Giudici, A. R. Goñi, C. Thomsen, P. G. Bolcatto, C. R. Proetto, and K. Eberl, Phys. Rev. B **70**, 235418 (2004).
[15] K. W. Edmonds *et al.*, Phys. Rev. Lett. **96**, 117207 (2006).
[16] H. Ohno *et al.*, Nature (London) **408**, 944 (2000).